

# Interaction between Metal and Graphene: Dependence on the Layer Number of Graphene

Jisook Lee,<sup>†</sup> Konstantin S. Novoselov,<sup>‡</sup> and Hyeon Suk Shin<sup>\*†</sup>

<sup>†</sup>Interdisciplinary School of Green Energy, Ulsan National Institute of Science and Technology (UNIST), Banyeon-ri 100, Ulsan 689-805, Korea, and <sup>‡</sup>School of Physics and Astronomy, University of Manchester, Oxford Road, Manchester, M13 9PL, U.K.

**ABSTRACT** The interaction between graphene and metal was investigated by studying the G band splitting in surface-enhanced Raman scattering (SERS) spectra of single-, bi-, and trilayer graphene. The Ag deposition on graphene induced large enhancement of the Raman signal of graphene, indicating SERS of graphene. In particular, the G band was split into two distinct peaks in the SERS spectrum of graphene. The extent of the G band splitting was  $13.0\text{ cm}^{-1}$  for single-layer,  $9.6\text{ cm}^{-1}$  for bilayer, and  $9.4\text{ cm}^{-1}$  for trilayer graphene, whereas the G band in the SERS spectrum of a thick multilayer was not split. The average SERS enhancement factor of the G band was 24 for single-layer, 15 for bilayer, and 10 for trilayer graphene. These results indicate that there is a correlation between SERS enhancement factor and the extent of the G band splitting, and the strongest interaction occurs between Ag and single-layer graphene. Furthermore, the Ag deposition on graphene can induce doping of graphene. The intensity ratio of 2D and G bands ( $I_{2D}/I_G$ ) decreased after Ag deposition on graphene, indicating doping of graphene. From changes in positions of G and 2D bands after the metal deposition on graphene, Ag deposition induced n-doping of graphene, whereas Au deposition induced p-doping.

**KEYWORDS:** graphene · Ag deposition · doping · surface-enhanced Raman scattering · Raman spectroscopy

One of important themes in recent graphene-based research is to investigate changes in physico-chemical properties of graphene as a function of the layer number.<sup>1,2</sup> The layer number of graphene affected the morphology of the metal deposited on graphene and the chemical reactivity of graphene. For example, the morphology of the Au film, including the grain size and the spacing between the grains when it was deposited on graphene, was strongly affected by the layer number of graphene, forming grains of a larger size and spacing in few-layer graphene compared to those in single-layer graphene.<sup>3</sup> Chemical reactivity of graphene has been investigated by its oxidation, which was measured by changes of  $I_D/I_G$  ratios in Raman spectra during heating to  $600\text{ }^\circ\text{C}$ . The  $I_D/I_G$  values decreased in the order single-, bi-, and trilayer graphene, indicating that single-layer graphene is more oxidized than bi- and trilayer graphene.<sup>4</sup> In the case of reactivity of graphene with

4-nitrobenzene diazonium salt, the single layer showed 10 times higher reactivity than the bi- or multilayer.<sup>5,6</sup>

Raman spectroscopy has been utilized as a powerful tool for the characterization of graphene, as it can identify the number of layers,<sup>7–10</sup> the electronic structure,<sup>11</sup> the edge structure,<sup>12</sup> the type of doping,<sup>13–17,35</sup> and any defects<sup>18,19</sup> in the graphene. Particularly, recent advance in Raman study of graphene has attracted much interest: obtaining resonance Raman spectra of R6G by using graphene as a fluorescence quencher<sup>20</sup> and enhancement of Raman signal of dyes on single-layer graphene *via* the chemical enhancement mechanism.<sup>21</sup> Furthermore, surface-enhanced Raman scattering (SERS) of mechanically exfoliated graphene and reduced graphene oxide has been studied in order to improve Raman signal.<sup>22–25</sup> However, dependence of SERS of graphene on the layer number has not been investigated in detail. In addition to SERS, binding of metal to graphene is also important for the research on graphene/metal composites and the interaction between graphene and metals.

Herein, we report the interaction between graphene and a metal. SERS spectra of single-, bi-, and trilayer graphene on which metal was deposited were measured. While the G band was split into two bands, the extent of the splitting decreased with increasing the number of graphene layers: single-layer > bilayer  $\geq$  trilayer. However, the G band in the SERS spectra of multilayer graphene (graphite) was not split. In particular, the SERS enhancement factor also decreased with increasing the number of graphene layers: single-layer > bilayer > trilayer. Thus, the splitting of the

\*Address correspondence to shin@unist.ac.kr.

Received for review November 6, 2010 and accepted December 15, 2010.

Published online December 21, 2010.  
10.1021/nn103004c

© 2011 American Chemical Society

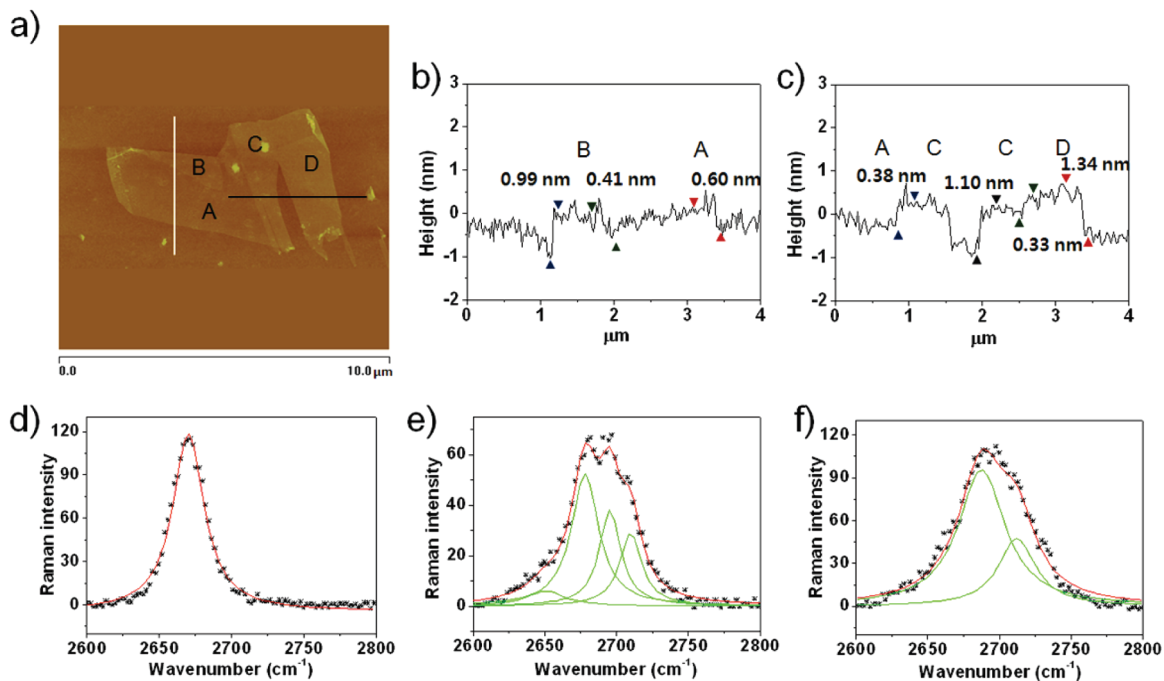


Figure 1. (a) AFM image and (b and c) height profile of graphene: (b) white line and (c) black line in AFM image. (d–f) 2D bands of the normal Raman spectra at each region: (d) single-layer for region A, (e) bilayer for regions B and C, and (f) trilayer for region D.

G band is assumed to be a factor determining the interaction between graphene and metal. Furthermore, doping of graphene with metal deposition was investigated from changes in  $I_{2D}/I_G$  ratios and shifts of the G and 2D bands.

## RESULTS AND DISCUSSION

Mechanically exfoliated graphene samples on a  $\text{SiO}_2$ (300 nm)/Si wafer were prepared by the procedure known as the scotch tape method.<sup>26,27</sup> The layer number of graphene can be identified by the thicknesses measured using AFM and the shape of the 2D band in the Raman spectra. As shown in Figure 1a–c, the AFM image indicates four regions with different thickness in the graphene sample: A (single-layer), B (bilayer), C (bilayer), and D (trilayer). These layers were confirmed again by the shape of the 2D band in the Raman spectrum of each region. Figure 1d–f shows that the 2D band in region A is well fitted with a single Lorentzian peak (single-layer), the 2D band in regions B and C with

four peaks (bilayer), and the 2D band in region D with two peaks (trilayer).<sup>7–9</sup>

Then, Ag of 4 nm thickness was deposited on the graphene sample by thermal evaporation, in which the Ag thickness was determined by a quartz crystal microbalance in a thermal evaporator. Ag was deposited in the form of nanoparticles. (See Figure S1.) Raman spectra of Ag-deposited graphene showed a larger Raman signal compared to those of as-prepared graphene, indicating that SERS occurs in Ag-deposited graphene.

Figure 2 shows normal Raman and SERS spectra of single-, bi-, and trilayer graphene before and after Ag deposition with a 532 nm excitation laser. SERS enhancement factors were calculated by comparing integrated intensities of the G and 2D bands before and after Ag deposition. The enhancement factors of the G and 2D bands are 24 and 16 for single-layer (Figure 2a), 15 and 12 for bilayer (Figure 2b), and 10 and 9 for trilayer (Figure 2c). It is particularly noted that the SERS

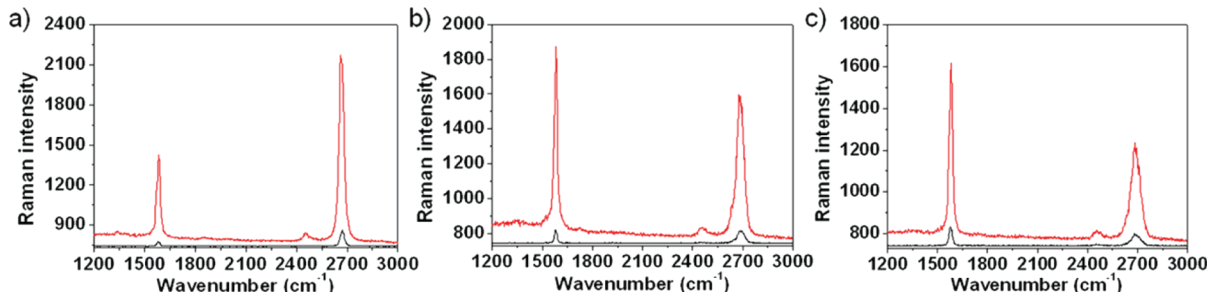
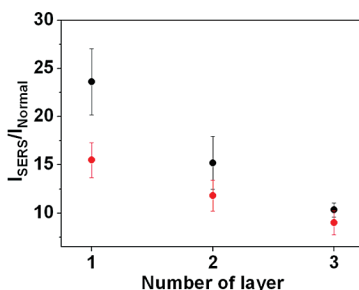


Figure 2. SERS spectra of (a) single-, (b) bi-, and (c) trilayer graphene before and after Ag deposition. Black curves are for normal Raman spectra before Ag deposition, and red curves are for SERS spectra after Ag deposition. A 532 nm laser was used for excitation with a laser power of 1.5 mW and an exposure time of 0.2 s.

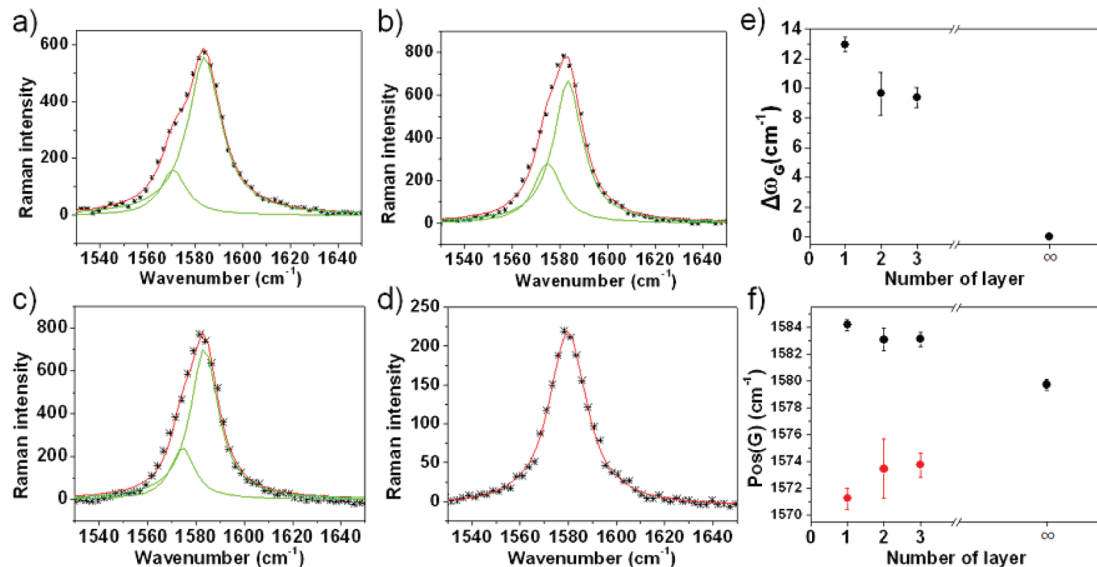


**Figure 3.** Enhancement factors of G and 2D bands calculated from integrated intensities of SERS and normal Raman spectra. Black and red circles indicate enhancement factors for the G band and 2D bands, respectively.

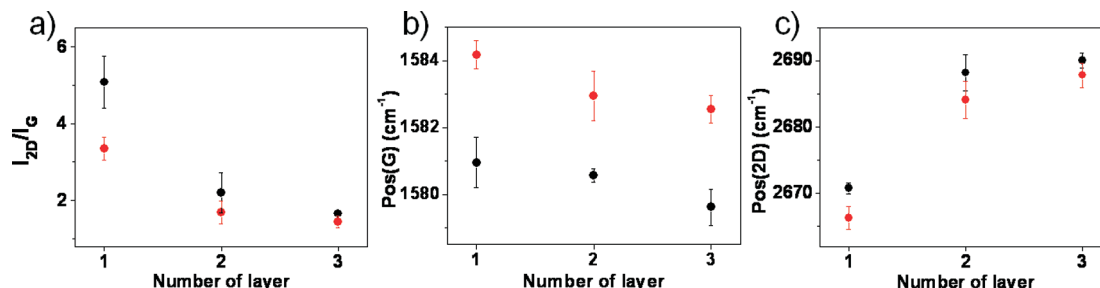
enhancement factor decreases with increasing the layer numbers. The change of the enhancement factor as a function of the number of layers is well shown in Figure 3 with error bars. This result is consistent with our previous result on SERS enhancement factors for single- and trilayer graphene by Au deposition.<sup>28</sup> The largest enhancement factor in single-layer graphene is thought to be due to the strong interaction between Ag and graphene. In the case of bi- and trilayer graphene, on the other hand, the interaction between Ag and graphene is assumed to be weak because of van der Waals interaction between the graphene layers, which may deteriorate the unique electron property of graphene. Such interaction between Ag and graphene will be further explained in the splitting of the G band and in the decrease of the  $I_{2D}/I_G$  ratio, indicating doping of graphene, later on.

Figure 4 illustrates the splitting of the G band after Ag deposition on the single-, bi-, and trilayer graphene and graphite. Before Ag deposition, the G band is observed around  $1580\text{ cm}^{-1}$  at any layer graphene. On the other hand, the G band of graphene after Ag deposition is split into two peaks at  $1571.2$  and  $1584.2\text{ cm}^{-1}$  for single-layer in Figure 4a, two peaks at  $1573.5$  and

$1583.1\text{ cm}^{-1}$  for bilayer in Figure 4b, and two peaks at  $1573.7$  and  $1583.1\text{ cm}^{-1}$  for trilayer graphene in Figure 4c. A prominent change in the G band after Ag deposition in Figure 4 is that the extent of the splitting of the G band decreases with increasing the number of layers. Specifically, the splitting of the G band is  $13.0\text{ cm}^{-1}$  for single-layer,  $9.6\text{ cm}^{-1}$  for bilayer, and  $9.4\text{ cm}^{-1}$  for trilayer, whereas the G band of graphite (thick multi-layer) is not split. It is noted that it is difficult to distinctly distinguish between the splittings in bi- and trilayer because they are within error margin. However, the trend of the decrement is observed with an increase in the number of graphene layers. The splitting of the G band can be attributed to the interaction between Ag and graphene, which induces a change in the graphene electronic structure. Dong et al. recently reported interaction between aromatic molecules and single-layer graphene, resulting in phonon symmetry breaking at the  $\Gamma$  point.<sup>29</sup> When tetrasodium 1,3,6,8-pyrenetetrasulfonic acid (TPA) was used as a dopant, it alters the electron density distribution of single-layer graphene and induces the G band splitting by lifting the 2-fold degeneracy of the LO and TO phonons. They also reported that the excitation-energy independence of the split G bands is in line with a first-order Raman process.<sup>29</sup> When Raman spectra of the Ag-deposited graphene samples in this study were obtained with a  $633\text{ nm}$  laser (Figure S2), the position of each split G band is almost the same as that in Figure 4 obtained with a  $533\text{ nm}$  laser, indicating that the Raman signal of Ag-deposited graphene is due to a first-order process. Since the interaction between Ag and graphene and the resulting changes in the graphene electronic structure were also theoretically proven by Giovannetti et al.,<sup>30</sup> our proposal on the G band splitting by the interaction between Ag and graphene seems to be reasonable. The splitting of the G band was identically ob-



**Figure 4.** (a–d) The deconvolved spectra of G bands after Ag deposition: (a) single-, (b) bi-, (c) trilayer graphene and (d) bulk graphite. (e) The difference of two fitted bands ( $\Delta\omega_G$ ) in a–d. (f) Frequencies of two fitted G bands in a–d.



**Figure 5.** Variation of  $I_{2D}/I_G$  before and after Ag deposition. (b and c) Positions of G and 2D bands before and after Ag deposition as a function of the layer number of graphene: (b) G and (c) 2D bands. Black and red circles indicate band positions before and after Ag deposition, respectively.

served for Au deposition and was larger in single-layer than in trilayer graphene (Figure S3).

Even though the 2D band is also sensitive to the number of graphene layers, the G band splitting was monitored in this study. The 2D band in the Raman spectrum of single-layer graphene could be split into two peaks after Ag deposition, whereas it was difficult to observe the splitting of the 2D bands in the Raman spectra of bi- and trilayer graphene because the 2D band could be deconvoluted to four peaks for bilayer and two peaks for trilayer before Ag deposition and the 2D band even after Ag deposition could be fitted with four peaks for bilayer and two peaks for trilayer, as shown in Figure S4.

From the above results, we found an interesting correlation between the extent of the G band splitting and the SERS enhancement factor. The order of the extent of the G band splitting in single-, bi-, and trilayer graphene is the same as that of the SERS enhancement factor: single-layer > bilayer > trilayer. Therefore, it is thought that the strongest interaction occurs between Ag and single-layer graphene.

The Ag deposition on graphene can induce doping of graphene. Indeed, variations of  $I_{2D}/I_G$  ratios and shifts of G and 2D bands are related to doping of graphene.<sup>13–15,31,32</sup> Figure 5a shows changes of  $I_{2D}/I_G$  ratios after Ag deposition in each graphene: from 5.1 (before Ag deposition) to 3.4 (after Ag deposition) for single-layer, from 2.2 to 1.7 for bilayer, from 1.7 to 1.4 for trilayer. This indicates that the  $I_{2D}/I_G$  ratio decreases after Ag deposition and the extent of the reduction in  $I_{2D}/I_G$  ratio is the largest in the single-layer. Thus, it is considered that single-layer graphene is highly doped with Ag deposition. Similarly, the decrease in  $I_{2D}/I_G$  ratios was reported for single- or multilayer graphene with adsorbed doping species such as tetracyanoethylene (TCNE) and tetrathiafulvalene (TTF),<sup>33</sup> various benzene derivatives,<sup>34</sup> aromatic molecules,<sup>35</sup> and halogen molecules.<sup>1</sup>

The type of doping can be determined from the position shift of the G and 2D bands.<sup>13,14,31</sup> It is known that the upshift of the G band position and the downshift of the 2D band position means n-doping of graphene, whereas the upshift of the G band position and the upshift of the 2D band position means p-doping.<sup>13,31</sup> In Figure 5b, the position of the G band shifts from  $1580.9 \text{ cm}^{-1}$  (before Ag deposition) to  $1584.2 \text{ cm}^{-1}$  (after Ag deposition) for single-layer, from  $1580.6 \text{ cm}^{-1}$  to  $1583.0 \text{ cm}^{-1}$  for bilayer, and from  $1579.6 \text{ cm}^{-1}$  to  $1582.5 \text{ cm}^{-1}$  for trilayer. (Spectra are shown in Figure S5.) On the other hand, the position of the 2D band shifts to lower wavenumber after Ag deposition by  $4.5 \text{ cm}^{-1}$  for single-layer, by  $4.1 \text{ cm}^{-1}$  for bilayer, and by  $2.2 \text{ cm}^{-1}$  for trilayer (Figure 5c). This result indicates n-doping of graphene with Ag deposition. Unlike Ag deposition, positions of both G and 2D bands shifted to high wavenumber when Au was deposited on graphene (Figure S6). This result indicates p-doping of graphene. The above results are consistent with the previous theoretical prediction that Ag- and Au-deposited graphene showed n- and p-type doping, respectively, due to the interaction between the metal and the graphene via an electron transfer driven by the work function difference.<sup>30</sup>

## CONCLUSIONS

In summary, the interaction between metal and graphene was studied by investigating SERS spectra, G band splitting, variation of  $I_{2D}/I_G$  ratio, and positions of G and 2D bands depending on the number of layers of graphene on which Ag was deposited. The SERS enhancement factors and the extent of G band splitting decreased with an increase in the number of graphene layers: single-layer > bilayer > trilayer. Furthermore, Ag deposition induced n-doping of graphene, whereas Au deposition induced p-doping. This study will open up new challenges for graphene-based electronics and composites.

## METHODS

**Preparation of Graphene Samples.** Graphene was mechanically exfoliated using Kish graphite from Toshiba Ceramics on a 300 nm  $\text{SiO}_2/\text{Si}$  substrate. The graphene layer is identified by AFM (Multimode V, Veeco Inc.) and Raman spectroscopy (Alpha 300S, WiTec GmbH). Ag was deposited on the graphene

samples at a rate of  $0.5 \text{ \AA/min}$  using a thermal evaporator (Woosung Hi-Vac).

**Characterization of Metal-Deposited Graphene.** Raman spectra were obtained using a micro-Raman system with a  $532 \text{ nm}$  excitation laser and a  $100\times$  objective lens ( $\text{NA} = 0.9$ ). The incident laser power is  $1.5 \text{ mW}$  and exposure time is  $0.2 \text{ s}$  to

avoid laser-induced thermal effects or damage. The normal and SERS spectra were fitted by Lorentzian single- and multipeak fitting.

**Acknowledgment.** This work was supported by the WCU (World Class University) program through the National Research Foundation funded by MEST of Korea (R31-2008-000-20012-0) and by KICOS through MEST in 2009 (No. 2009-00591).

**Supporting Information Available:** AFM image of graphene after Ag deposition, the splitting of the G band in Figure 4 at 633 nm, the difference of the G band after Au deposition in Figure 4e, and the position of G and 2D bands before and after Au deposition in Figure 5b and c. This material is available free of charge via the Internet at <http://pubs.acs.org>.

## REFERENCES AND NOTES

- Jung, N.; Kim, N.; Jockusch, S.; Turro, N. J.; Kim, P.; Brus, L. Charge Transfer Chemical Doping of Few Layer Graphenes: Charge Distribution and Band Gap Formation. *Nano Lett.* **2009**, *9*, 4133–4137.
- Pollak, E.; Geng, B.; Jeon, K.-J.; Lucas, I. T.; Richardson, T. J.; Wang, F.; Kostecki, R. The Interaction of Li<sup>+</sup> with Single-Layer and Few-Layer Graphene. *Nano Lett.* **2010**, *10*, 3386–3388.
- Zhou, H.; Qui, C.; Liu, Z.; Yang, H.; Hu, L.; Li, J.; Yang, H.; Gu, C.; Sun, L. Thickness-Dependent Morphologies of Gold on N-Layer Graphenes. *J. Am. Chem. Soc.* **2010**, *132*, 944–946.
- Liu, L.; Ryu, S.; Tomasik, M. R.; Stolyarova, E.; Jung, N.; Hybertsen, M. S.; Steigerwald, M. L.; Brus, L. E.; Flynn, G. W. Graphene Oxidation: Thickness-Dependent Etching and Strong Chemical Doping. *Nano Lett.* **2008**, *8*, 1965–1970.
- Sharma, R.; Sharma, Baik, J. H.; Perera, C. J.; Strano, M. S. Anomalously Large Reactivity of Single Graphene Layers and Edges toward Electron Transfer Chemistries. *Nano Lett.* **2010**, *10*, 398–405.
- Koehler, F. M.; Jacobsen, A.; Ensslin, K.; Stampfer, C.; Stark, W. J. Selective Chemical Modification of Graphene Surfaces: Distinction between Single- and Bilayer Graphene. *Small* **2010**, *6*, 1125–1130.
- Ferrari, A. C.; Meyer, J. C.; Scardaci, V.; Casiraghi, C.; Lazzari, M.; Mauri, F.; Piscanec, S.; Jiang, D.; Novoselov, K. S.; Roth, S.; et al. Raman Spectrum of Graphene and Graphene Layers. *Phys. Rev. Lett.* **2006**, *97*, 187401.
- Hao, Y.; Wang, Y.; Wang, L.; Ni, Z.; Wang, Z.; Wang, R.; Koo, C. K.; Shen, Z.; Thong, J. T. L. Probing Layer Number and Stacking Order of Few-Layer Graphene by Raman Spectroscopy. *Small* **2010**, *6*, 195–200.
- Wang, Y.; Ni, Z.; Yu, T.; Shen, Z. X.; Wang, H.; Wu, Y.; Chen, W.; A. Wee, T. S. Raman Studies of Monolayer Graphene: The Substrate Effect. *J. Phys. Chem. C* **2008**, *112*, 10637–10640.
- Park, J. S.; Reina, A.; Saito, R.; Kong, J.; Dresselhaus, G.; Dresselhaus, M. S. G' Band Raman Spectra of Single, Double and Triple Layer Graphene. *Carbon* **2009**, *47*, 1303–1310.
- Malard, L. M.; Nilsson, J.; Elias, D. C.; Plentz, J. C.; Alves, E. S.; Castro Neto, A. H.; Pimenta, M. A. Probing the Electronic Structure of Bilayer Graphene by Raman Scattering. *Phys. Rev. B* **2007**, *76*, 201401.
- You, Y.; Ni, Z.; Yu, T.; Shen, Z. Edge Chirality Determination of Graphene by Raman Spectroscopy. *Appl. Phys. Lett.* **2008**, *93*, 163112.
- Das, A.; Pisana, S.; Chakraborty, B.; Piscanec, S.; Saha, S. K.; Waghmare, U. V.; Novoselov, K. S.; Krishnamurthy, H. R.; Geim, A. K.; Ferrari, A. C.; et al. Monitoring Dopants by Raman Scattering in an Electrochemically Top-Gated Graphene Transistor. *Nature Nanotechnol.* **2008**, *3*, 210–215.
- Shi, Y.; Dong, X.; Chen, P.; Wang, J.; Li, L.-J. Effective Doping of Single-Layer Graphene from Underlying SiO<sub>2</sub> Substrates. *Phys. Rev. B* **2009**, *79*, 115402.
- Stampfer, C.; Molitor, F.; Graf, D.; Ensslin, K.; Jungen, A.; Hierold, C.; Wirtz, L. Raman Imaging of Doping Domains in Graphene on SiO<sub>2</sub>. *Appl. Phys. Lett.* **2007**, *91*, 241907.
- Casiraghi, C.; Pisana, S.; Novoselov, K. S.; Geim, A. K.; Ferrari, A. C. Raman Fingerprint of Charged Impurities in Graphene. *Appl. Phys. Lett.* **2007**, *91*, 233108.
- Wei, D.; Liu, Y.; Wang, Y.; Zhang, H.; Huang, L.; Yu, G. Synthesis of N-Doped Graphene by Chemical Vapor Deposition and Its Electrical Properties. *Nano Lett.* **2009**, *9*, 1752–1758.
- Liu, H.; Ryu, S.; Chen, Z.; Steigerwald, M. L.; Nuckolls, C.; Brus, L. E. Photochemical Reactivity of Graphene. *J. Am. Chem. Soc.* **2009**, *131*, 17099–17101.
- Jorio, A.; Lucchese, M. M.; Stavale, F.; Ferreira, E. H. M.; Moutinho, M. V. O.; Capaz, R. B.; Achete, C. A. Raman Study of Ion-Induced Defects in N-layer Graphene. *J. Phys.: Condens. Matter.* **2010**, *22*, 334204.
- Xie, L.; Ling, X.; Fang, Y.; Zhang, J.; Liu, Z. Graphene as a Substrate to Suppress Fluorescence in Resonance Raman Spectroscopy. *J. Am. Chem. Soc.* **2009**, *131*, 9890–9891.
- Ling, X.; Xie, L.; Fang, Y.; Xu, H.; Zhang, H.; Kong, J.; Dresselhaus, M. S.; Zhang, J.; Liu, Z. Can Graphene be Used as a Substrate for Raman Enhancement. *Nano Lett.* **2010**, *10*, 553–561.
- Xu, C.; Wang, X. Fabrication of Flexible Metal-Nanoparticle Films Using Graphene Oxide Sheets as Substrates. *Small* **2009**, *5*, 2212–2217.
- Gao, L.; Ren, W.; Liu, B.; Saito, R.; Wu, Z.-S.; Li, S.; Jiang, C.; Li, F.; Cheng, H.-M. Surface and Interference Coenhanced Raman Scattering of Graphene. *ACS Nano* **2009**, *3*, 933–939.
- Fu, X.; Bei, F.; Wang, X.; O'Brien, S.; Lombardi, J. R. Excitation Profile of Surface-Enhanced Raman Scattering in Graphene-Metal Nanoparticle Based Derivatives. *Nanoscale* **2010**, *1*, 1461–1466.
- Schedin, F.; Lidorikis, E.; Lombardo, A.; Kravets, V. G.; Geim, A. K.; Grigorenko, A. N.; Novoselov, K. S.; Ferrari, A. C. Surface-Enhanced Raman Spectroscopy of Graphene. *ACS Nano* **2010**, *4*, 5617–5626.
- Novoselov, K. S.; Geim, A. K.; Morozov, S. V.; Jiang, D.; Zhang, Y.; Dubonos, S. V.; Grigorieva, I. V.; Firsov, A. A. Electric Field Effect in Atomically Thin Carbon Films. *Science* **2004**, *306*, 666.
- Novoselov, K. S.; Jiang, D.; Schedin, F.; Booth, T. J.; Khotkevich, V. V.; Morozov, S. V.; Geim, A. K. Two-Dimensional Atomic Crystals. *Proc. Natl. Acad. Sci. U. S. A.* **2005**, *102*, 10451.
- Lee, J.; Shim, S.; Kim, B.; Shin, H. S. Surface-Enhanced Raman Scattering of Single- and Few-Layer Graphene by the Deposition of Gold Nanoparticles. *Chem. – Eur. J.*, accepted.
- Dong, X.; Shi, Y.; Zhao, Y.; Chen, D.; Ye, J.; Yao, Y.; Gao, F.; Ni, Z.; Yu, T.; Shen, Z.; et al. Symmetry Breaking of Graphene Monolayer by Molecular Decoration. *Phys. Rev. Lett.* **2009**, *102*, 135501.
- Giovannetti, G.; Khomyakov, P. A.; Brocks, G.; Karpan, V. M.; Brink, J.; Kelly, P. J. Doping Graphene with Metal Contacts. *Phys. Rev. Lett.* **2008**, *101*, 026803.
- Pisana, S.; Lazzari, M.; Casiraghi, C.; Novoselov, K. S.; Geim, A. K.; Ferrari, A. C.; Mauri, F. Breakdown of the Adiabatic Born-Oppenheimer Approximation in Graphene. *Nat. Mater.* **2007**, *6*, 198–201.
- Basko, D. M.; Piscanec, S.; Ferrari, A. C. Electron-Electron Interactions and Doping Dependence of the Two-Phonon Raman Intensity in Graphene. *Phys. Rev. B* **2009**, *80*, 165413.
- Voggu, R.; Das, B.; Rout, C. S.; Rao, C. N. R. Effects of Charge Transfer Interaction of Graphene with Electron Donor and Acceptor Molecules Examined using Raman Spectroscopy and Cognate Techniques. *J. Phys.: Condens. Matter* **2008**, *20*, 472204.
- Das, B.; Voggu, R.; Rout, C. S.; Rao, C. N. R. Changes in the Electronic Structure and Properties of Graphene Induced by Molecular Charge-Transfer. *Chem. Commun.* **2008**, 5155–5157.
- Dong, X.; Fu, D.; Fang, W.; Shi, Y.; Chen, P.; Li, L.-J. Doping Single-Layer Graphene with Aromatic Molecules. *Small* **2009**, *5*, 1422–1426.